



Published in final edited form as:

*Circ Cardiovasc Imaging*. 2012 January 1; 5(1): 94–101. doi:10.1161/CIRCIMAGING.111.966424.

## Molecular Imaging of Mesenchymal Stem Cell: Mechanistic Insight into Cardiac Repair following Experimental Myocardial Infarction

Jingxiong Wang, MD, PhD, Amer Najjar, PhD, Sui Zhang, MD, PhD, Brian Rabinovich, PhD, James T. Willerson, MD, Juri G. Gelovani, MD, PhD, and Edward T. H. Yeh, MD

Texas Heart Institute at St. Luke's Episcopal Hospital (J.W., J.T.W., E.T.H.Y.); the Departments of Cardiology (S.Z., E.T.H.Y.) and the Experimental Diagnostic Imaging (A.N., B.R., J.G.G.), The University of Texas-M. D. Anderson Cancer Center, Houston, Texas.

### Abstract

**Background**—Mesenchymal stem cells (MSCs) can differentiate into endothelial cells *in vivo*. However, it is unknown if the differentiated MSCs persist *in vivo* and if this potential persistence contributes to functional improvement following experimental myocardial infarction (EMI).

**Methods and Results**—We generated a lentivector encoding two distinct reporter genes, one driven by a constitutive murine stem cell virus promoter and the other, by an endothelial specific Tie-2 promoter. The endothelial specificity of the lentivector was validated by its expression in endothelial cells, but not in human MSCs (hMSCs). The lentivirus-transduced hMSCs were injected into peri-infarct areas of the hearts of severe combined immune-deficient mice. Persistence of injected cells was tracked by bioluminescence imaging (BLI) and verified by immunohistochemical staining (IHS). The BLI signal from the endothelial-specific reporter revealed that hMSCs differentiated into endothelial cells 48 hours following injection. However, both the constitutive and the endothelial-specific BLI signals disappeared by day 50. Nonetheless, the improvement in left ventricle ejection fraction with hMSC therapy persisted for up to 6 months. IHS showed that hMSC-derived endothelial cells integrated into endogenous CD31<sup>+</sup> vessels. Furthermore, hMSC-transplanted hearts had more CD31<sup>+</sup> vessels and a lesser degree of cardiac fibrosis compared to the controls at 6 months.

**Conclusions**—hMSCs differentiated into endothelial cells and integrated into blood vessels after EMI. The differentiated hMSCs only lasted for up to 50 days *in vivo*, but improvement in cardiac function persisted for up to 6 months. Increased angiogenesis and decreased fibrosis were associated with cardiac functional improvement following hMSC transplantation.

### Keywords

molecular imaging; mesenchymal stem cell; endothelial differentiation

---

**Correspondence to:** Edward T.H. Yeh, MD, University of Texas-M.D. Anderson Cancer Center, 1400 Pressler Blvd, Box 1451, Houston, TX 77030, USA. Phone: (713) 792-1960, Fax: (713) 745-1942; etyeh@mdanderson.org.

**Publisher's Disclaimer:** This is a PDF file of an unedited manuscript that has been accepted for publication. As a service to our customers we are providing this early version of the manuscript. The manuscript will undergo copyediting, typesetting, and review of the resulting proof before it is published in its final citable form. Please note that during the production process errors may be discovered which could affect the content, and all legal disclaimers that apply to the journal pertain.

This work was presented in part at the American Heart Association Scientific Sessions, Orlando, FL, November 14–18, 2009, and published in abstract form (*Circulation*. 2009;120:S754–S755).

Stem cell therapy for cardiovascular disease has been studied for over a decade.<sup>1-3</sup> Preclinical studies have demonstrated that the mesenchymal stem cells (MSCs) facilitate both myocardial repair and neovascularization in animal models of cardiac injury.<sup>4-7</sup> Human clinical trials have also validated the safety and efficacy of MSC therapy in patients with acute myocardial infarction (MI) and heart failure.<sup>8-12</sup> Endothelial cell differentiation and the paracrine effect have been proposed to be responsible for the efficacy of MSC therapy. However, it is not known if differentiated MSCs persist *in vivo* and if this potential persistence contributes to functional improvement following experimental MI (EMI). To determine the long-term fate of transplanted MSCs *in vivo* by imaging, we generated a lentivector encoding two distinct double fusion reporter genes (DFR). One DFR, GFP/firefly-luciferase (G/f-Luc) is controlled by an endothelial specific promoter Tie-2,<sup>13</sup> and the other DFR, mCherry/renilla luciferase (C/r-Luc) is driven by the constitutively active U3 region from the murine stem cell virus-long terminal repeat (MSCV-LTR). This lentivector is designed to (a) track the long-term survival and proliferation of the injected hMSCs in the infarcted hearts and (b) determine whether hMSC undergo endothelial differentiation and if so, the kinetics of such. Combined bioluminescent imaging (BLI), fluorescent imaging and cardiac MRI demonstrated that injected hMSCs differentiate into endothelial cells in the injured hearts. However, the injected hMSCs persisted for only a limited time, suggesting that the long-term functional improvement after EMI is due to paracrine effects.

## Methods

### Endothelial Cell-Specific Vector Construction and Lentiviral Packaging

The Tie-2 promoter was utilized to drive the expression of the G/f-Luc to facilitate endothelial cell-specific imaging. We first generated a bidirectional lentiviral dual expression vector, pLVD430-C/r-Luc-G/f-Luc, in which the constitutive expression of C/r-Luc and G/f-Luc DFR is controlled by the MSCV and human phosphoglycerate kinase (hPGK) promoters, respectively. We then modified the vector by replacing hPGK with the Tie-2 promoter. Briefly, the Tie-2 promoter was amplified by PCR from T2HpGFPT2I5/XK (kindly provided by Thomas Sato, Cornell University) using primers designed to bind the regions flanking the promoter and containing *BstBI* and *ScaI* restriction sites (underlined), respectively: forward: 5'-TAATTTCGAATCACACAGGAAACAGCTATGAC-3'; reverse: 5'-TAATAGTACTCGACGTTGTAAAACGACGGCCAGTG-3'. The final expression vector was produced by removing the PGK promoter via digestion of pLVD430-C/r-Luc-G/f-Luc with *HpaI* and *BstBI* and replacing it with the Tie-2 promoter, a 2kb *ScaI/BstBI*-digested PCR product.

Lentiviral packaging, concentrating, and titering were performed as previously described.<sup>14-15</sup>

### Cell Culture and Lentiviral Transduction

hMSCs (Lonza, Walkersville, MD) were cultured in supplemented MSCGM™ medium according to manufacturer specifications. Mouse cardiac endothelial cells (mETCs, Cedarlane, Burlington, NC) were cultured in DMEM supplemented with 10% serum at 30°C. hMSCs and mETCs (at passage 3 to 6) were transduced with concentrated lentivirus at a multiplicity of infection of 30. The transduction efficiencies were assessed by measuring constitutive mCherry expression in hMSCs. The Tie-2 endothelial specific expression in the mETCs was validated by measuring GFP expression via fluorescent microscopy (FM) and flow cytometry (FACS, BLR-II, BD Biosciences, CA). Constitutive expression vs. endothelial specific expression was determined by measuring BLI intensity of r-Luc and f-Luc with a Xenogen IVIS 200 system (Caliper LS) as described previously.<sup>16-17</sup> The ratio of BLI signal and cell number was determined by plating serially diluted cells ( $1 \times 10^3$  to

$1 \times 10^5$  cells) in a 24-well plate and quantifying signal intensities in each well. The data was expressed as photons/second/cell.

### **Induction of MI, Injection of hMSCs, in vivo BLI Tracking of Injected hMSCs, and Cardiac Functional Assessment**

All animal studies were approved by the Institutional Animal Care and Use Committees of the University of Texas M.D. Anderson Cancer Center. Female severe combined immunodeficient (SCID) mice (C3H, 16–20 g; Jackson Laboratory, Bar Harbor, Maine) were used in all *in vivo* studies. MI was induced as previously described.<sup>18</sup> After MI induction,  $5 \times 10^5$  lentivirus-transduced hMSCs were injected in 25–30  $\mu$ L of basal medium directly into the peri-infarcted areas of each heart. Control mice were injected with basal medium only. Each group consisted of 10 mice.

*In vivo* BLI was longitudinally performed using the same Xenogen IVIS system at different time points. Five minutes prior to imaging, each mouse received via tail vein 100  $\mu$ L of 40 mg/ml coelentraxine (CLTZ) for detection of the constitutive BLI/r-Luc signal, indicating the total injected hMSC population, or a 100- $\mu$ L intra-peritoneal injection of 125 mg/kg D-luciferin for assessment of the inducible BLI/f-Luc signal, indicating endothelial differentiation of injected hMSCs.<sup>16–17</sup> To circumvent interference between BLI/r-Luc and BLI/f-Luc signals, the measurements were recorded six hours apart.

To assess cardiac function, a 7.0 T Biospec small animal scanner (Bruker Biospin Inc., Billerica, MA) was used to scan the mice longitudinally before (baseline) and after (week 1 and months 1, 2, 3, and 6) injection of the transduced hMSCs; the left ventricle ejection fraction (LVEF) was calculated as described previously.<sup>18</sup> All measurements were conducted in a blinded fashion to ensure impartial interpretation.

### **Preparation of Single Cell Suspension from Hearts and Cell Staining for FACS Analysis**

Three mice in each group were sacrificed 2 weeks after hMSCs/medium injection. The hearts were collected, and single cell suspensions were obtained by collagenase II (Worthington Biochemical Corporation, NJ) digestion. The isolated cells were washed, fixed, permeabilized, and then incubated with monoclonal anti-cardiac troponin T (cTn-T, 1:200, clone 1A11; Advanced Immunochemical, CA), or with a polyclonal anti-VE cadherin (1:100, Bender MedSystems, CA) for 50 minutes at 4°C. The secondary antibody was conjugated with Alexa Fluor 633 or with Alexa Fluor 488 (Molecular Probes, OR), respectively. After three washes, all cells were incubated with PE-conjugated anti-human HLA-ABC (Cedarlane Laboratories, NC) for 30 minutes before FACS analysis.

### **Immunohistochemistry**

Freshly excised tissues were immersed in OCT, frozen in liquid nitrogen, and stored at  $-80^\circ\text{C}$  until use. OCT embedded mouse hearts were sectioned to 5  $\mu$ m, collected on slides and frozen at  $-80^\circ\text{C}$  until staining.

For GFP and CD31 protein staining, heart sections were fixed with 3.7% paraformaldehyde (pH 7.4) at 4°C for 5 minutes immediately before staining, rinsed in PBS three times, and blocked at room temperature for 30 minutes in PBS containing 5% horse serum. Sections were then incubated with primary antibodies anti-CD31 (Abcam, CA) or anti-GFP (Clontech, CA) at room temperature for one hour. The sections were rinsed three times and incubated with the secondary antibodies (Alexa Fluor 488-conjugated goat anti-mouse IgG and Alexa Fluor 568 rabbit anti-rat, Invitrogen, CA) at room temperature for 45 minutes. Paired primary and secondary antibodies were used for double staining. The slides were rinsed in PBS three times before adding mounting medium containing DAPI (Vector Labs,

CA). FM was used to quantify vessel density by counting and averaging the number of vessels per field based on 6 fields (400X magnified) randomly chosen from the border zone of each heart section.

For measurement of cardiac fibrosis, we chosen 16 sections at 350  $\mu\text{m}$  intervals spanning the entire length of the heart from a total of 1100 sections<sup>19</sup> for Masson Trichrome approach as described.<sup>20</sup> The cardiac fibrosis area ( $\text{mm}^2$ ) in each section was performed by staining and scanning the stained areas at 10 $\times$  magnification and quantifying ImageJ (NIH). The areas of perivascular fibrosis in arteries and veins were excluded from the measurements. The total fibrotic volume ( $\text{mm}^3$ ) in each heart was calculated from the sum of areas of fibrosis ( $A_1+A_2+\dots+A_{16}$ ) multiplied by 0.35.

## Statistics

We used SPSS Smart Viewer 15.0 (SPSS, Chicago, Ill) for statistical analysis of the data. Repeated-measures ANOVA was used for comparison of LVEF between control and hMSCs groups. Continuous data were analyzed by Mann-Whitney test between 2 groups or by 1-way ANOVA test with Bonferroni post hoc analysis for more than 2 groups. All data collection and analyses were performed in a blinded fashion.

## Results

### Validation of Constitutive and Endothelial-Specific Dual Reporter Lentivector

Using FM and FACS analysis, we determined that the average transduction efficiency of the U3/Tie-2 containing lentivector was  $93.4 \pm 5.8\%$  for mETCs (Figures 1B and 1D), and  $4 \pm 6.3\%$  for hMSCs (Figures 1C and 1E), respectively. Importantly, FM, FACS analysis, and *in vitro* BLI demonstrated that mETCs expressed both constitutive r-Luc and endothelial specific f-Luc, whereas hMSCs expressed only r-Luc (Figure 1F). A robust linear correlation was observed between the number of transduced hMSCs and photon flux (Figure 1G), which allowed us to quantify precisely the BLI *in vivo* measurements.

### Persistence and Differentiation of hMSC following experimental MI

The transduced hMSCs were injected into the peri-infarct regions of SCID mice following EMI as previously described.<sup>21-22</sup> As shown in Figure 2A, all BLI signals are located in the chest, indicating that injected hMSCs did not migrate to peripheral organs in sufficient numbers to be detected. Endothelial-specific BLI/f-Luc signal was detectable at day two (Figures 2A (lower row) and 2B). Furthermore, both constitutive BLI/r-Luc and BLI/f-Luc signals declined gradually one week post-injection and disappeared completely at day 60 days. These observations suggested that the majority of hMSCs did not survive in the recipient hearts for longer than two months whether differentiated or not. Using immunofluorescent microscopy, we observed that  $\text{GFP}^+/\text{CD31}^+$  cells, which represented differentiated hMSCs, resided in the border zone of infarcted hearts and some of these cells were juxtaposed to endogenous endothelial cells (Figures 2C and 2D). FACS illustrated an increase in  $\text{HLA-ABC}^+/\text{VE-cadherin}^+$  cells, which represented hMSC-derived endothelial cells in hearts following hMSC injection, in comparison to medium injection (1.2% versus 0.1%, Figure 2E).

### Improvement in Cardiac Function in the Infarcted Hearts after hMSC Injection

We used cardiac MRI to evaluate the therapeutic benefit of hMSC injection (Figure 3). End-systolic (ES) and end-diastolic (ED) volumes, measured longitudinally for up to 6 months, were used to calculate LVEFs (Figure 3A). One week after EMI, the decreases in LVEFs were similar in both the control and hMSCs-injected groups (Figure 3B), suggesting that our EMI protocol was carried out consistently and achieved a similar degree of cardiac damage

in both groups. However, there was a statistically significant improvement in LVEFs in the hMSC-treated group in comparison to the control group, beginning at one month following EMI (Figure 3B). The improvement in LVEFs in the hMSCs-treated animals was sustained for up to 6 months (Figure 3A and 3B). Overall, hMSC therapy produced a 10% net improvement in LVEF ( $p < 0.05$ ). No animals died in the two groups during the 6-month observation period.

### Structural Changes Following hMSC Injection

Although implanted hMSCs were detected in the hearts for less than 2 months, the improvement in cardiac function lasted for up to 6 months. To examine the mechanisms that may account for this long-term functional improvement, we measured the number of CD31<sup>+</sup> vessels in the border zone and quantified fibrotic volume of the hearts at 2 weeks and at 6 months following hMSC treatment. As shown in Figures 4A and 4B, the overall number of CD31<sup>+</sup> vessels was significantly greater in the hMSC treated hearts than in control hearts ( $p < 0.05$ ). Moreover, there was a significant increase in vessel density in hMSCs injected hearts that was associated with this overall increase in total vessel number at both 2 weeks (83 versus 94/field,  $p < 0.05$ ) and 6 months (69 versus 113/field,  $p < 0.01$ ). Likewise, cardiac fibrosis was significantly diminished in the hMSC treated hearts in comparison to the controls (Figures 4C and 4D, 3.41 versus 2.09 mm<sup>3</sup>/heart,  $p < 0.05$ ), although at 2 weeks post-injection, the degree of cardiac fibrosis was not different between these two groups. These results suggest that enhanced endogenous angiogenesis and attenuated fibrosis may be responsible for long-term improvement in cardiac function following hMSC therapy.

## Discussion

### Long-Term Survival, Efficacy of MSC Therapy and Underlying Mechanisms

MSC treatment has been shown to be significantly protective against MI-associated heart damage by decreasing infarct size and reducing ventricular remodeling in short-term (less than two months) studies in a variety of animal models. However, the long-term (six months or longer) effects have not been rigorously investigated and the outcomes from limited reports are not consistent.<sup>23–24</sup> In the present study, intramyocardial delivery of hMSCs into the peri-infarct zones of SCID mouse hearts resulted in long-term (6 months) therapeutic benefits as demonstrated by improvement in LVEF, decrease in fibrosis, and increase in vessel density in infarcted hearts. Teratoma formation in the hMSC-treated animals was not observed over the 6 month monitoring period, suggesting that this therapeutic strategy is potentially safe.

In our hands, hMSCs survived in the infarcted hearts for less than 50 days. Thus, the long-term therapeutic benefits cannot be directly ascribed to the short-term persistence of the injected hMSCs.

The longevity of MSCs is not consistent from study to study. Dai *et al.* reported that in a rat acute MI model, cardiac functional improvement was observed at 4 weeks after MSC transplantation. At 6 months, the therapeutic benefits were lost, although the injected cells were still observed in the all tested time points.<sup>23</sup> Using a swine acute MI model, Jameel *et al.* demonstrated that treatment with a bone marrow-derived multipotent progenitor cells (MPC) population, a major proportion of which are MSCs, resulted in improvement in LVEF as early as 10 days after MI, and persisted to 4 months without significant MPC engraftment.<sup>18</sup> In a human heart transplantation study, the MSCs of donor origin remained present in the heart for 6 years after transplantation, and maintained cardiomyogenic and osteogenic differentiation capacity.<sup>24</sup> In a separate clinical study, van der Bogt *et al.* compared the *in vivo* behavior of both adipose and bone marrow derived MSC in the



infarcted hearts, and found that neither of these cell types restored cardiac function.<sup>25</sup> The differences in cell source, species, experimental or clinical protocol, and potential differences in the disease model prevent direct comparison among the various investigations.<sup>10, 12, 26</sup>

In this study, we used *in vivo* BLI to ascertain the viability of the injected hMSCs and used cardiac MRI to assess LVEF. Compared to other imaging modalities, BLI is more sensitive and specific and can be performed in small live animals (e.g. mice).<sup>27</sup> This approach allowed us to collect longitudinal *in vivo* imaging data, thereby avoiding sampling biases that can occur with the use of multiple animals sacrificed at different time points for conventional histological staining. Moreover, the signal intensity is dynamically correlated with the original number of injected hMSCs and can be used to track engraftment and proliferation of transplanted cells. It should be noted, however, that bioluminescence signals do not automatically equate to cell survival because of detection limits. Using BLI, investigators in several labs have accurately tracked the fate of injected human CD34<sup>+</sup> cells, and adipose- and bone marrow-derived MSCs in the mouse heart after EMI.<sup>18, 25</sup> Using the same strategy, we demonstrated that bioluminescent detection of the injected hMSCs began to dissipate 1 week after injection and could not be detected beyond 50 days. Furthermore, using immunofluorescent microscopy, we determined that MSCs differentiated into endothelial cells and integrated into the wall of blood vessels.

The therapeutic benefits of hMSC implantation cannot be directly attributed to the endothelial differentiation of hMSCs since a small subset of the cells undergoes differentiation. Therefore, the observed therapeutic benefits, manifested in increased vessel density and reduced fibrosis, are more likely to be attributed to paracrine effects exerted by factors released by hMSC.<sup>28</sup> Numerous studies support the paracrine-mediated therapeutic effects of MSCs on damaged myocardium through the secretion of protective factors that promote angiogenesis and attenuate fibrosis. Conditioned media from hypoxia-exposed Akt-expressing MSCs has been shown to protect rat cardiomyocytes grown under hypoxia and reduce infarct size in a rodent model.<sup>29</sup> Moreover, MSCs secrete angiogenic factors such as VEGF, bFGF, and HGF that promote neovascularization,<sup>30-31</sup> and downregulation of VEGF expression in MSCs has been shown to reduce myocardial recovery.<sup>32</sup> MSC transplantation into ischemic rat myocardium has also been shown to reduce fibrosis and increase myocardial thickness, improving cardiac function without concomitant myocardial regeneration.<sup>33</sup> MSCs can downregulate extracellular tissue remodeling in a paracrine manner by inducing myocardial expression of collagen I and III and tissue inhibitor of metalloproteinase-1 and by decreasing MMP-2 and MMP-9 expression.<sup>34</sup> The paracrine therapeutic effect can also be manifested in the induction of endogenous cardiac progenitor cells differentiation via MSC-secreted BMPs and FGF, modulators of cardiac cell differentiation.<sup>35</sup>

### **In Vivo Detection of hMSC Differentiation into Endothelial Cells in the Infarcted Myocardium**

There is accumulating evidence that MSCs can differentiate into cardiac endothelial and smooth muscle cells under a variety of *in vitro* conditions.<sup>10, 12, 26, 36-37</sup> However, confirmation of such *in vivo* has been hampered by limited availability of non-invasive modalities. In this study, we created a lentiviral reporter in which two sets of DFR genes, *C/r-Luc*, controlled by the constitutive promoter MSCV, and *G/f-Luc*, driven by the endothelial specific promoter Tie-2. We showed that there is robust constitutive *C/r-Luc* expression in both hMSCs and mETCs *in vitro*. As expected, *G/f-Luc* expression was only observed in mETCs. Consistent with the *in vitro* observation, undifferentiated hMSCs, when injected into the infarcted hearts, underwent endothelial differentiation, as demonstrated by robust *f-Luc* expression in the injected areas. We validated our bioluminescent results using

IFM. Importantly, using CD31 staining and cardiac MRI, we found that endothelial differentiation correlated with the formation of blood vessels in the peri-infarct zones and an improvement in LVEF, respectively. The endothelial inducible BLI signal reached maximum 1 week after injection, and disappeared with the constitutive BLI signal at day 50. The concurrent regression of both tissue-specific and constitutive BLI signals implies a decline in implanted cell population survival.

### MSCs and Cardiac Repair

Growing evidence suggests that the therapeutic benefit of MSCs appears to be mediated predominantly via paracrine-mediated effects, rather than direct regeneration of various cardiac cells by differentiation.<sup>12, 27, 31, 38–42</sup> In this study, we found that, injected hMSCs differentiated into endothelial cells during the early stages (1–2 weeks post injection) as determined by the presence of HLA-ABC<sup>+</sup>/CD31<sup>+</sup> cells that reside in the peri-infarct regions. A few of them even integrated into the wall of newly formed vessels. In agreement with other reports, our finding suggests that at an early stage following transplantation, hMSC may play a role in creating new vessels. Thus, our findings support the notion that abolishing MSC-derived angiogenesis at the early stage may adversely affect the repair process.<sup>43</sup> We observed that only a small number of HLA-ABC<sup>+</sup>/CD31<sup>+</sup> cells were detected in the injected heart sections and that the differentiated endothelial cells survived in the damaged heart for less than 50 days. Conversely, the increase in vessel density, and the decrease in fibrosis persisted up to 6 months and paralleled long-term functional improvement. Thus, it is more likely that the injected hMSCs trigger endogenous repair mechanisms. These may include release of various paracrine factors and cytokines that may prevent the adverse inflammation caused by cardiac infarction, and stimulation of repair processes.

### Acknowledgments

We thank Dr James A. Bankson, Chenghui Ren and Allan Prejusa for their excellent technical assistance, Dr. Michele A. Zacks for her editorial assistance.

#### Sources of Funding

This work was supported in part by NIH grant # R01 HL086983 (to J.G.G., E.T.H.Y.). J.W. is the recipient of a Research Fellowship from the Canadian Institutes of Health Research. E.T.H.Y. is the McNair Scholar at the Texas Heart Institute. The Authors would also like to acknowledge support from the Cancer Center Support Grant (P30-CA016672, PI: Ronald A. DePinho) and the Experimental Cancer Imaging Research Program (U24-CA126577, PI: John D. Hazle).

#### Disclosures

Dr Gelovani received an honoraria payment from Takeda Foundation; and holds a consultant membership of Macrocylics and Sib Tech, separately.

### References

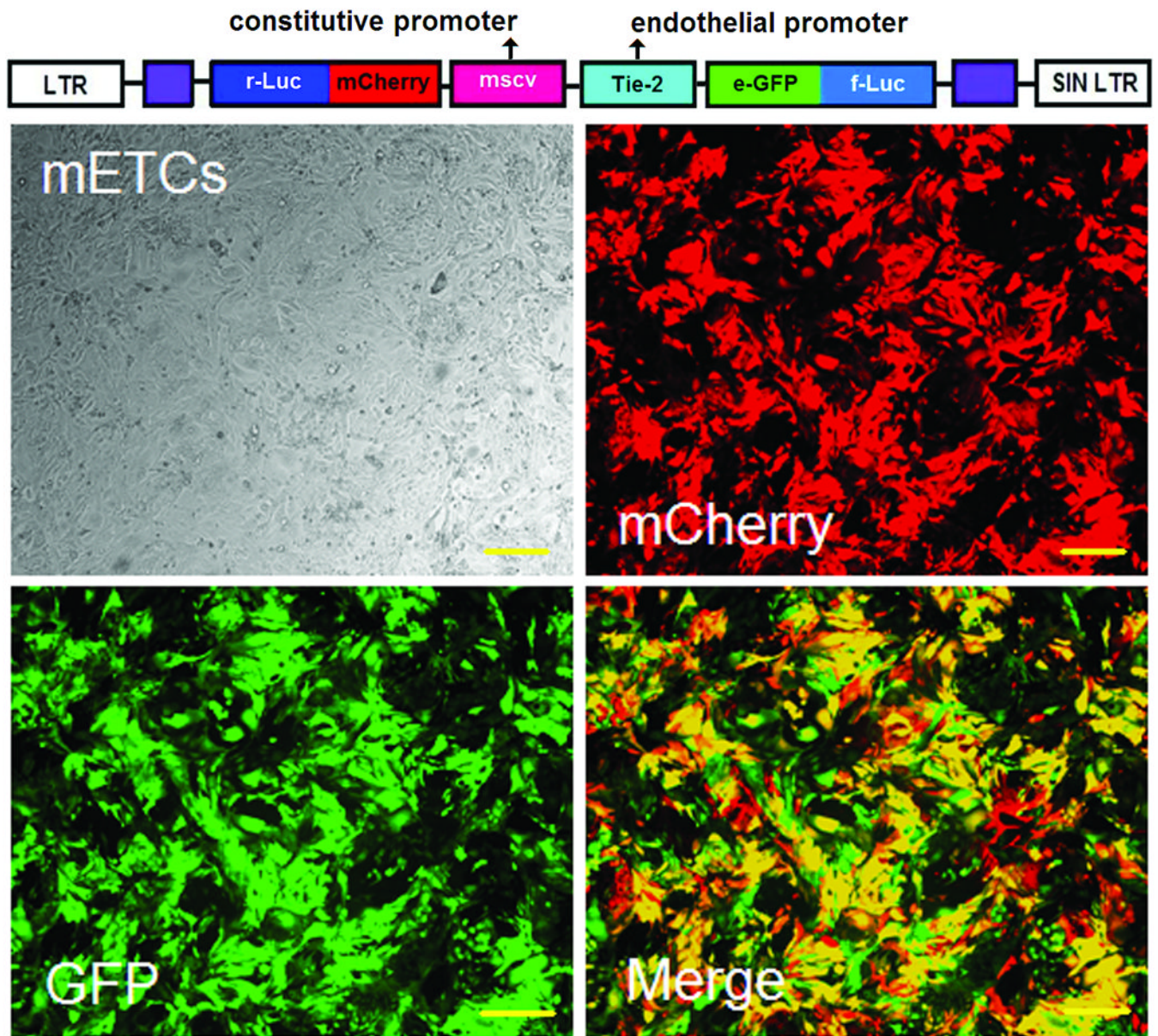
1. Wollert KC, Drexler H. Cell therapy for the treatment of coronary heart disease: a critical appraisal. *Nat Rev Cardiol.* 2010; 7:204–215. [PubMed: 20177405]
2. Janssens S. Stem cells in the treatment of heart disease. *Annu Rev Med.* 2010; 61:287–300. [PubMed: 20059339]
3. George JC. Stem cell therapy in acute myocardial infarction: a review of clinical trials. *Transl Res.* 2010; 155:10–19. [PubMed: 20004357]
4. Amado LC, Schuleri KH, Saliaris AP, Boyle AJ, Helm R, Oskouei B, Centola M, Eneboe V, Young R, Lima JA, Lardo AC, Heldman AW, Hare JM. Multimodality noninvasive imaging demonstrates in vivo cardiac regeneration after mesenchymal stem cell therapy. *J Am Coll Cardiol.* 2006; 48:2116–2124. [PubMed: 17113001]

5. Miyahara Y, Nagaya N, Kataoka M, Yanagawa B, Tanaka K, Hao H, Ishino K, Ishida H, Shimizu T, Kangawa K, Sano S, Okano T, Kitamura S, Mori H. Monolayered mesenchymal stem cells repair scarred myocardium after myocardial infarction. *Nat Med*. 2006; 12:459–465. [PubMed: 16582917]
6. Silva GV, Litovsky S, Assad JA, Sousa AL, Martin BJ, Vela D, Coulter SC, Lin J, Ober J, Vaughn WK, Branco RV, Oliveira EM, He R, Geng YJ, Willerson JT, Perin EC. Mesenchymal stem cells differentiate into an endothelial phenotype, enhance vascular density, and improve heart function in a canine chronic ischemia model. *Circulation*. 2005; 111:150–156. [PubMed: 15642764]
7. Toma C, Pittenger MF, Cahill KS, Byrne BJ, Kessler PD. Human mesenchymal stem cells differentiate to a cardiomyocyte phenotype in the adult murine heart. *Circulation*. 2002; 105:93–98. [PubMed: 11772882]
8. Chugh AR, Zuba-Surma EK, Dawn B. Bone marrow-derived mesenchymal stems cells and cardiac repair. *Minerva Cardioangiol*. 2009; 57:185–202. [PubMed: 19274029]
9. Noort WA, Feye D, Van Den Akker F, Stecher D, Chamuleau SA, Sluijter JP, Doevendans PA. Mesenchymal stromal cells to treat cardiovascular disease: strategies to improve survival and therapeutic results. *Panminerva Med*. 2010; 52:27–40. [PubMed: 20228724]
10. Paul D, Samuel SM, Maulik N. Mesenchymal stem cell: present challenges and prospective cellular cardiomyoplasty approaches for myocardial regeneration. *Antioxid Redox Signal*. 2009; 11:1841–1855. [PubMed: 19260767]
11. Salem HK, Thiemermann C. Mesenchymal stromal cells: current understanding and clinical status. *Stem Cells*. 2010; 28:585–596. [PubMed: 19967788]
12. Trivedi P, Tray N, Nguyen T, Nigam N, Gallicano GI. Mesenchymal stem cell therapy for treatment of cardiovascular disease: helping people sooner or later. *Stem Cells Dev*. 2010; 19:1109–1120. [PubMed: 20092388]
13. Sato TN, Qin Y, Kozak CA, Audus KL. Tie-1 and tie-2 define another class of putative receptor tyrosine kinase genes expressed in early embryonic vascular system. *Proc Natl Acad Sci U S A*. 1993; 90:9355–9358. [PubMed: 8415706]
14. Rabinovich B, Li J, Wolfson M, Lawrence W, Beers C, Chalupny J, Hurren R, Greenfield B, Miller R, Cosman D. NKG2D splice variants: a reexamination of adaptor molecule associations. *Immunogenetics*. 2006; 58:81–88. [PubMed: 16470377]
15. van Laake LW, Passier R, Monshouwer-Kloots J, Nederhoff MG, Ward-van Oostwaard D, Field LJ, van Echteld CJ, Doevendans PA, Mummery CL. Monitoring of cell therapy and assessment of cardiac function using magnetic resonance imaging in a mouse model of myocardial infarction. *Nature protocols*. 2007; 2:2551–2567.
16. Kidd S, Spaeth E, Dembinski JL, Dietrich M, Watson K, Klopp A, Battula VL, Weil M, Andreeff M, Marini FC. Direct evidence of mesenchymal stem cell tropism for tumor and wounding microenvironments using in vivo bioluminescent imaging. *Stem Cells*. 2009; 27:2614–2623. [PubMed: 19650040]
17. Wurdinger T, Badr C, Pike L, de Kleine R, Weissleder R, Breakefield XO, Tannous BA. A secreted luciferase for ex vivo monitoring of in vivo processes. *Nat Methods*. 2008; 5:171–173. [PubMed: 18204457]
18. Jameel MN, Li Q, Mansoor A, Qiang X, Sarver A, Wang X, Swingen C, Zhang J. Long-term functional improvement and gene expression changes after bone marrow-derived multipotent progenitor cell transplantation in myocardial infarction. *Am J Physiol Heart Circ Physiol*. 2010; 298:H1348–H1356. [PubMed: 20173039]
19. Michael LH, Ballantyne CM, Zachariah JP, Gould KE, Pocius JS, Taffet GE, Hartley CJ, Pham TT, Daniel SL, Funk E, Entman ML. Myocardial infarction and remodeling in mice: effect of reperfusion. *Am J Physiol*. 1999; 277:H660–H668. [PubMed: 10444492]
20. Zeisberg EM, Tarnavski O, Zeisberg M, Dorfman AL, McMullen JR, Gustafsson E, Chandraker A, Yuan X, Pu WT, Roberts AB, Neilson EG, Sayegh MH, Izumo S, Kalluri R. Endothelial-to-mesenchymal transition contributes to cardiac fibrosis. *Nat Med*. 2007; 13:952–961. [PubMed: 17660828]
21. Wang J, Zhang S, Rabinovich B, Bidaut L, Soghomonyan S, Alauddin MM, Bankson JA, Shpall E, Willerson JT, Gelovani JG, Yeh ET. Human CD34<sup>+</sup> cells in experimental myocardial infarction:

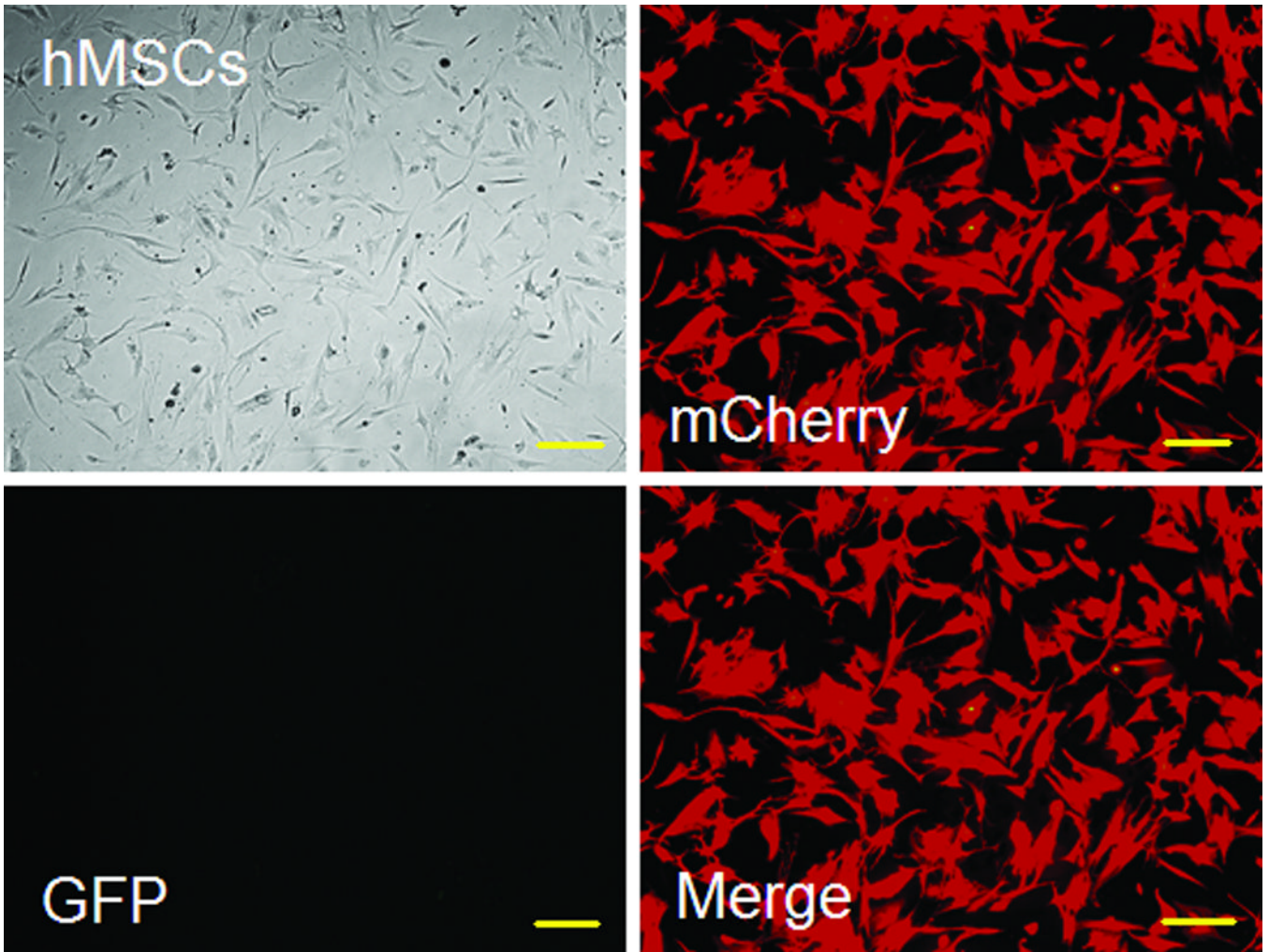


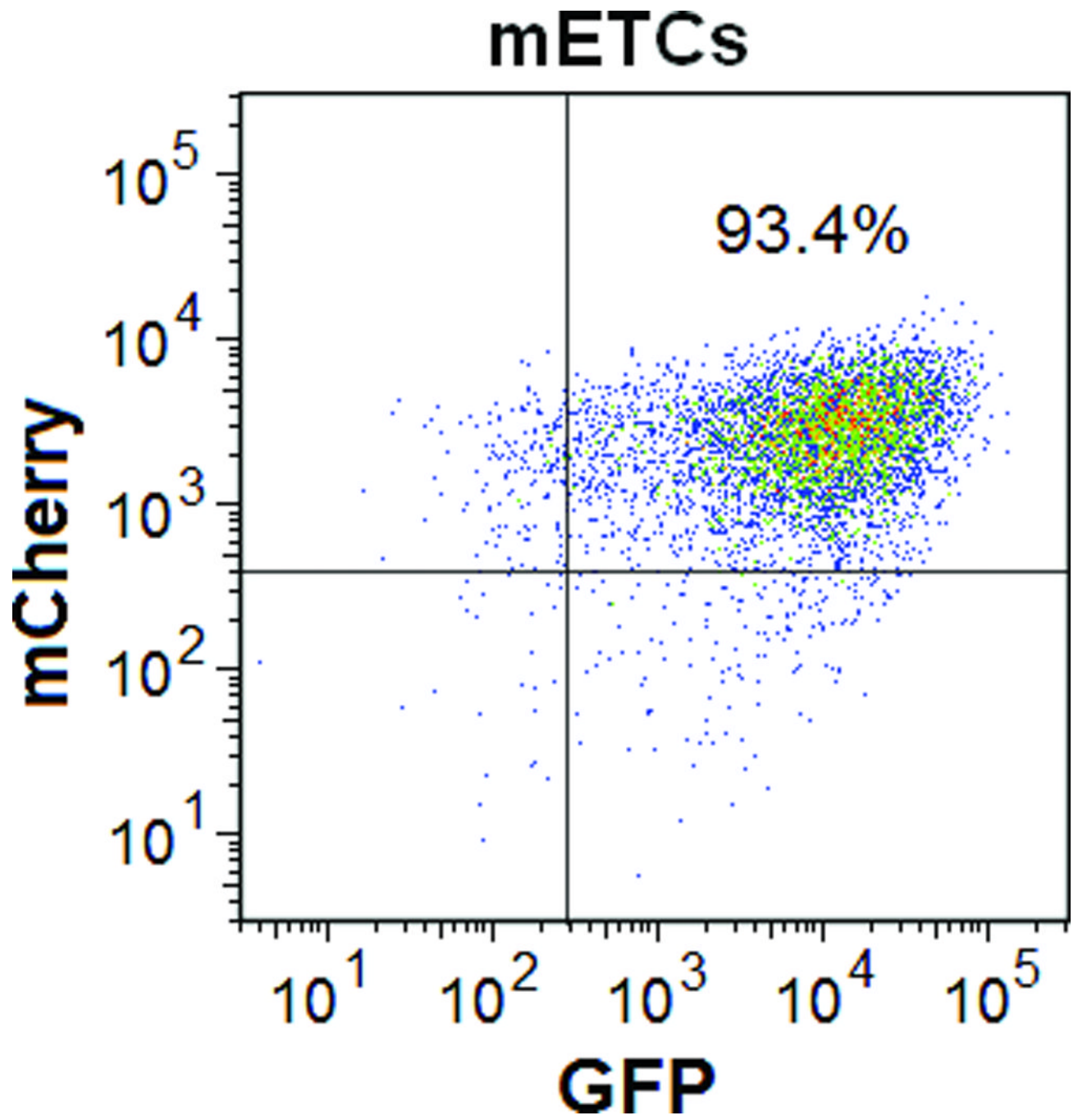
- long-term survival, sustained functional improvement, and mechanism of action. *Circ Res.* 2010; 106:1904–1911. [PubMed: 20448213]
22. Yeh ET, Zhang S, Wu HD, Korbling M, Willerson JT, Estrov Z. Transdifferentiation of human peripheral blood CD34<sup>+</sup>-enriched cell population into cardiomyocytes, endothelial cells, and smooth muscle cells in vivo. *Circulation.* 2003; 108:2070–2073. [PubMed: 14568894]
  23. Dai W, Hale SL, Martin BJ, Kuang JQ, Dow JS, Wold LE, Kloner RA. Allogeneic mesenchymal stem cell transplantation in postinfarcted rat myocardium: short- and long-term effects. *Circulation.* 2005; 112:214–223. [PubMed: 15998673]
  24. Hoogduijn MJ, Crop MJ, Peeters AM, Korevaar SS, Eijken M, Drabbels JJ, Roelen DL, Maat AP, Balk AH, Weimar W, Baan CC. Donor-derived mesenchymal stem cells remain present and functional in the transplanted human heart. *Am J Transplant.* 2009; 9:222–230. [PubMed: 18976299]
  25. van der Bogt KE, Schrepfer S, Yu J, Sheikh AY, Hoyt G, Govaert JA, Velotta JB, Contag CH, Robbins RC, Wu JC. Comparison of transplantation of adipose tissue- and bone marrow-derived mesenchymal stem cells in the infarcted heart. *Transplantation.* 2009; 87:642–652. [PubMed: 19295307]
  26. Psaltis PJ, Zannettino AC, Worthley SG, Gronthos S. Concise review: mesenchymal stromal cells: potential for cardiovascular repair. *Stem Cells.* 2008; 26:2201–2210. [PubMed: 18599808]
  27. Rabinovich BA, Ye Y, Etto T, Chen JQ, Levitsky HI, Overwijk WW, Cooper LJ, Gelovani J, Hwu P. Visualizing fewer than 10 mouse T cells with an enhanced firefly luciferase in immunocompetent mouse models of cancer. *Proc Natl Acad Sci U S A.* 2008; 105:14342–14346. [PubMed: 18794521]
  28. Loffredo FS, Steinhauser ML, Gannon J, Lee RT. Bone marrow-derived cell therapy stimulates endogenous cardiomyocyte progenitors and promotes cardiac repair. *Cell Stem Cell.* 2011; 8:389–398. [PubMed: 21474103]
  29. Gnecci M, He H, Noiseux N, Liang OD, Zhang L, Morello F, Mu H, Melo LG, Pratt RE, Ingwall JS, Dzau VJ. Evidence supporting paracrine hypothesis for Akt-modified mesenchymal stem cell-mediated cardiac protection and functional improvement. *FASEB J.* 2006; 20:661–669. [PubMed: 16581974]
  30. Dzau VJ, Gnecci M, Pachori AS, Morello F, Melo LG. Therapeutic potential of endothelial progenitor cells in cardiovascular diseases. *Hypertension.* 2005; 46:7–18. [PubMed: 15956118]
  31. Kinnaird T, Stabile E, Burnett MS, Lee CW, Barr S, Fuchs S, Epstein SE. Marrow-derived stromal cells express genes encoding a broad spectrum of arteriogenic cytokines and promote in vitro and in vivo arteriogenesis through paracrine mechanisms. *Circ Res.* 2004; 94:678–685. [PubMed: 14739163]
  32. Markel TA, Wang Y, Herrmann JL, Crisostomo PR, Wang M, Novotny NM, Herring CM, Tan J, Lahm T, Meldrum DR. VEGF is critical for stem cell-mediated cardioprotection and a crucial paracrine factor for defining the age threshold in adult and neonatal stem cell function. *Am J Physiol Heart Circ Physiol.* 2008; 295:H2308–H2314. [PubMed: 18849336]
  33. Berry MF, Engler AJ, Woo YJ, Pirolli TJ, Bish LT, Jayasankar V, Morine KJ, Gardner TJ, Discher DE, Sweeney HL. Mesenchymal stem cell injection after myocardial infarction improves myocardial compliance. *Am J Physiol Heart Circ Physiol.* 2006; 290:H2196–H2203. [PubMed: 16473959]
  34. Ohnishi S, Sumiyoshi H, Kitamura S, Nagaya N. Mesenchymal stem cells attenuate cardiac fibroblast proliferation and collagen synthesis through paracrine actions. *FEBS Lett.* 2007; 581:3961–3966. [PubMed: 17662720]
  35. Ling L, Nurcombe V, Cool SM. Wnt signaling controls the fate of mesenchymal stem cells. *Gene.* 2009; 433:1–7. [PubMed: 19135507]
  36. Davani S, Marandin A, Mersin N, Royer B, Kantelip B, Herve P, Etievent JP, Kantelip JP. Mesenchymal progenitor cells differentiate into an endothelial phenotype, enhance vascular density, and improve heart function in a rat cellular cardiomyoplasty model. *Circulation.* 2003; 108 Suppl 1:II253–II258. [PubMed: 12970242]

37. Duffy GP, Ahsan T, O'Brien T, Barry F, Nerem RM. Bone marrow-derived mesenchymal stem cells promote angiogenic processes in a time- and dose-dependent manner in vitro. *Tissue Eng Part A*. 2009; 15:2459–2470. [PubMed: 19327020]
38. Boyle AJ, McNiece IK, Hare JM. Mesenchymal stem cell therapy for cardiac repair. *Methods Mol Biol*. 2010; 660:65–84. [PubMed: 20680813]
39. Gneocchi M, Zhang Z, Ni A, Dzau VJ. Paracrine mechanisms in adult stem cell signaling and therapy. *Circ Res*. 2008; 103:1204–1219. [PubMed: 19028920]
40. Ladage D, Brixius K, Steingen C, Mehlhorn U, Schwinger RH, Bloch W, Schmidt A. Mesenchymal stem cells induce endothelial activation via paracrine mechanisms. *Endothelium*. 2007; 14:53–63. [PubMed: 17497361]
41. Schafer R, Northoff H. Cardioprotection and cardiac regeneration by mesenchymal stem cells. *Panminerva Med*. 2008; 50:31–39. [PubMed: 18427386]
42. Tolar J, Le Blanc K, Keating A, Blazar BR. Concise review: hitting the right spot with mesenchymal stromal cells. *Stem Cells*. 2010; 28:1446–1455. [PubMed: 20597105]
43. Yoon CH, Koyanagi M, Iekushi K, Seeger F, Urbich C, Zeiher AM, Dimmeler S. Mechanism of improved cardiac function after bone marrow mononuclear cell therapy: role of cardiovascular lineage commitment. *Circulation*. 2010; 121:2001–2011. [PubMed: 20421519]

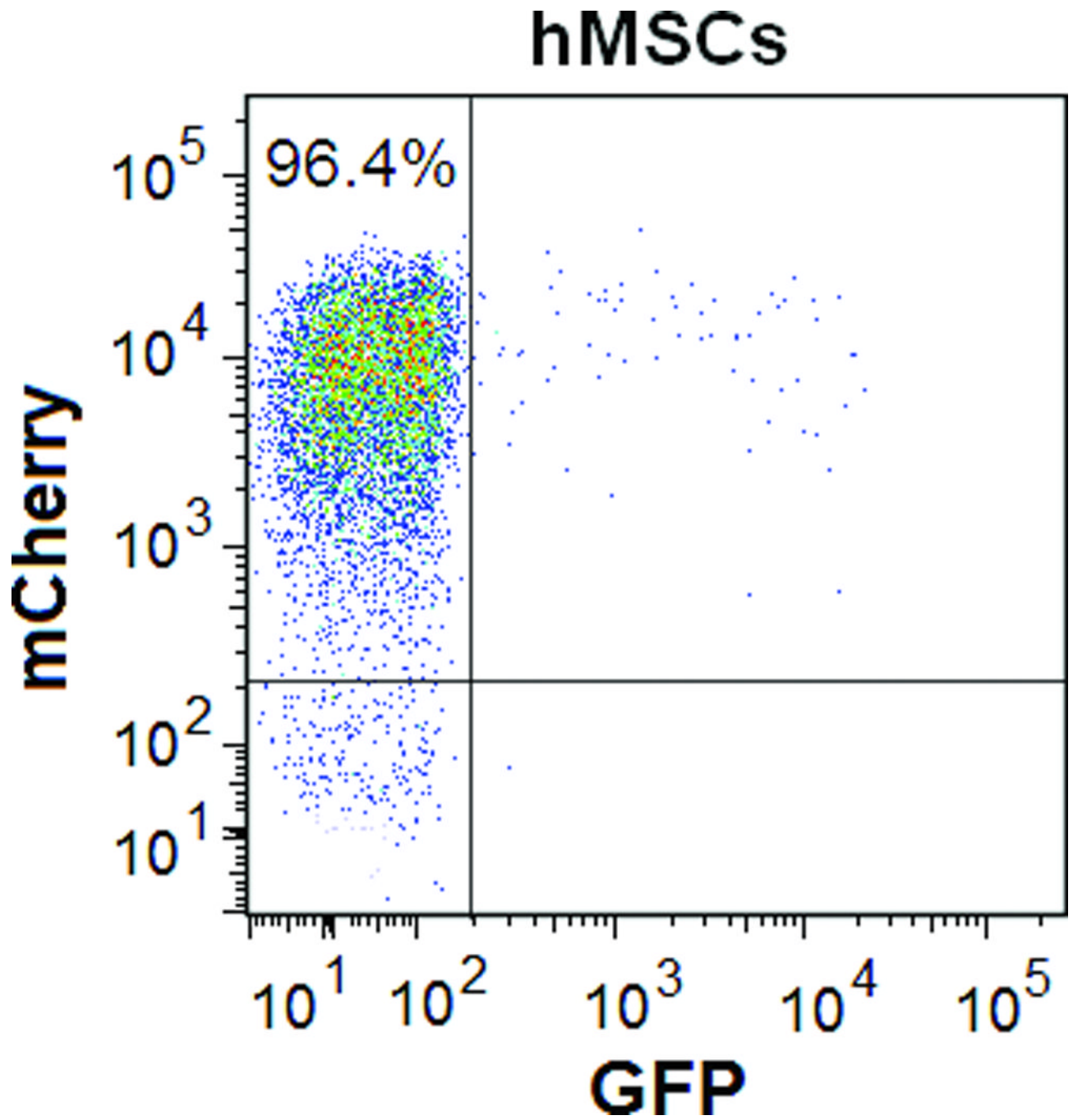


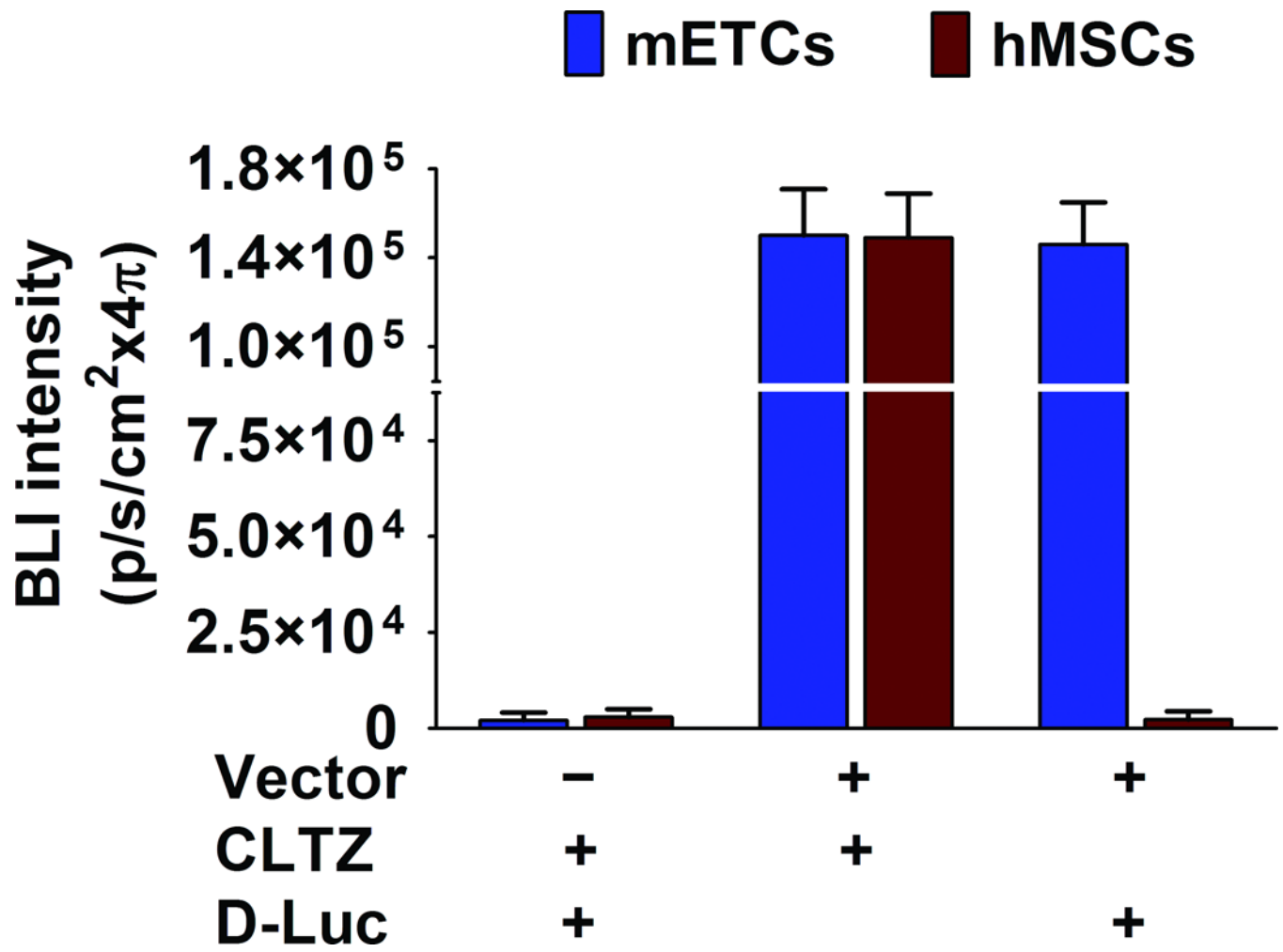


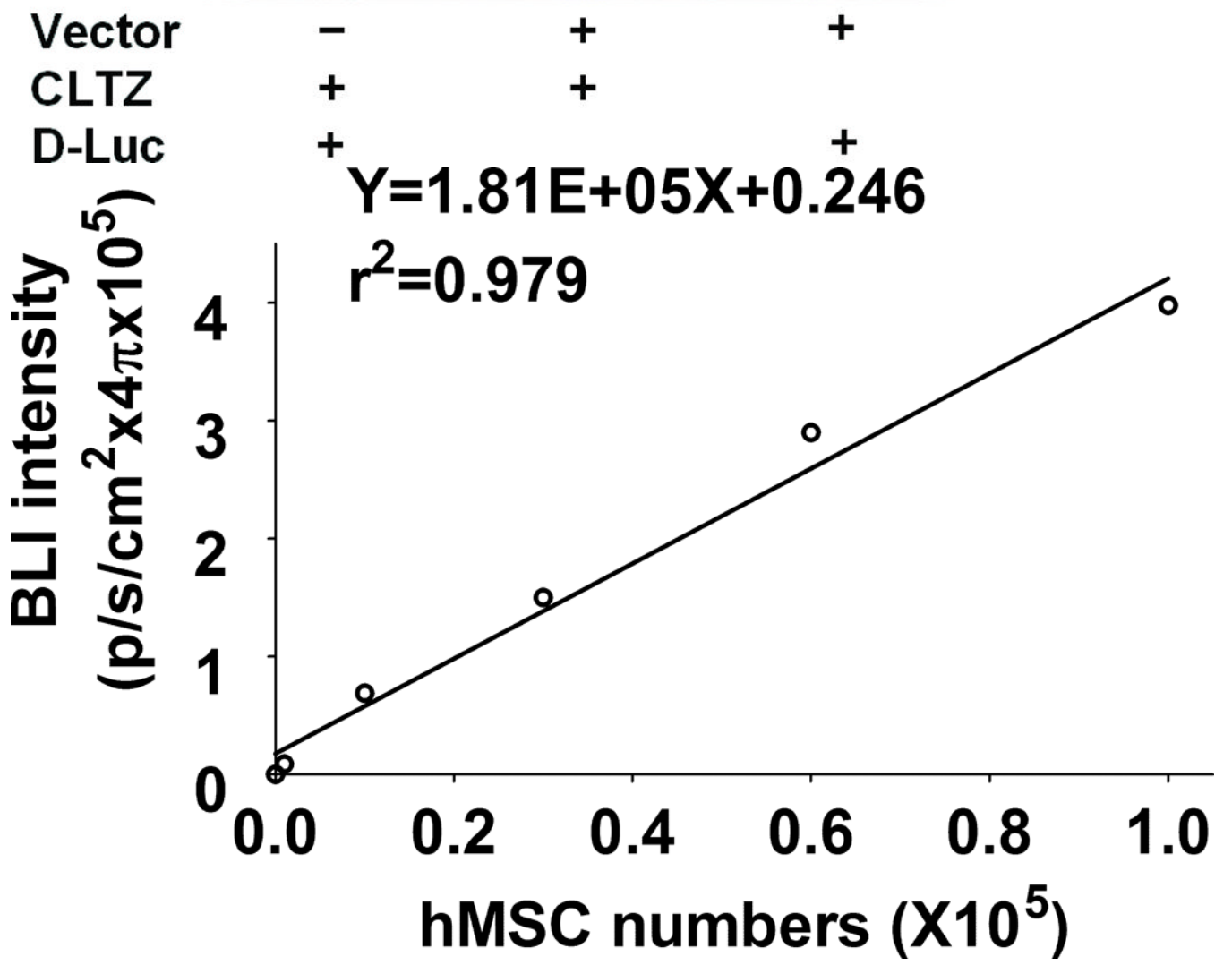
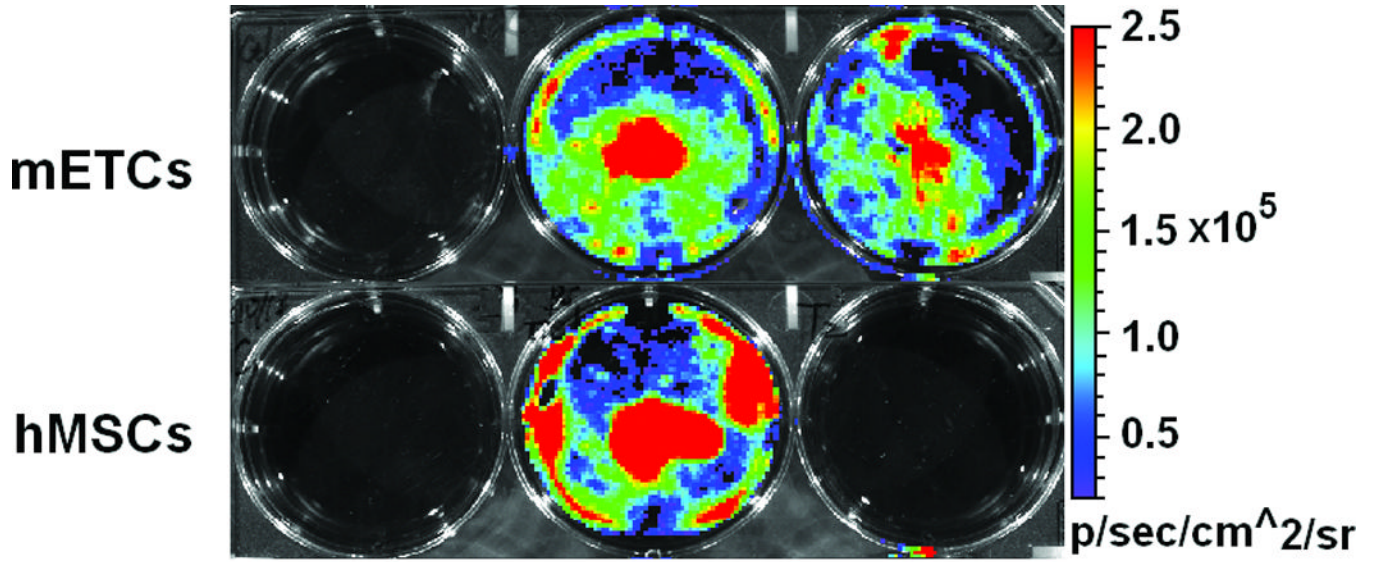


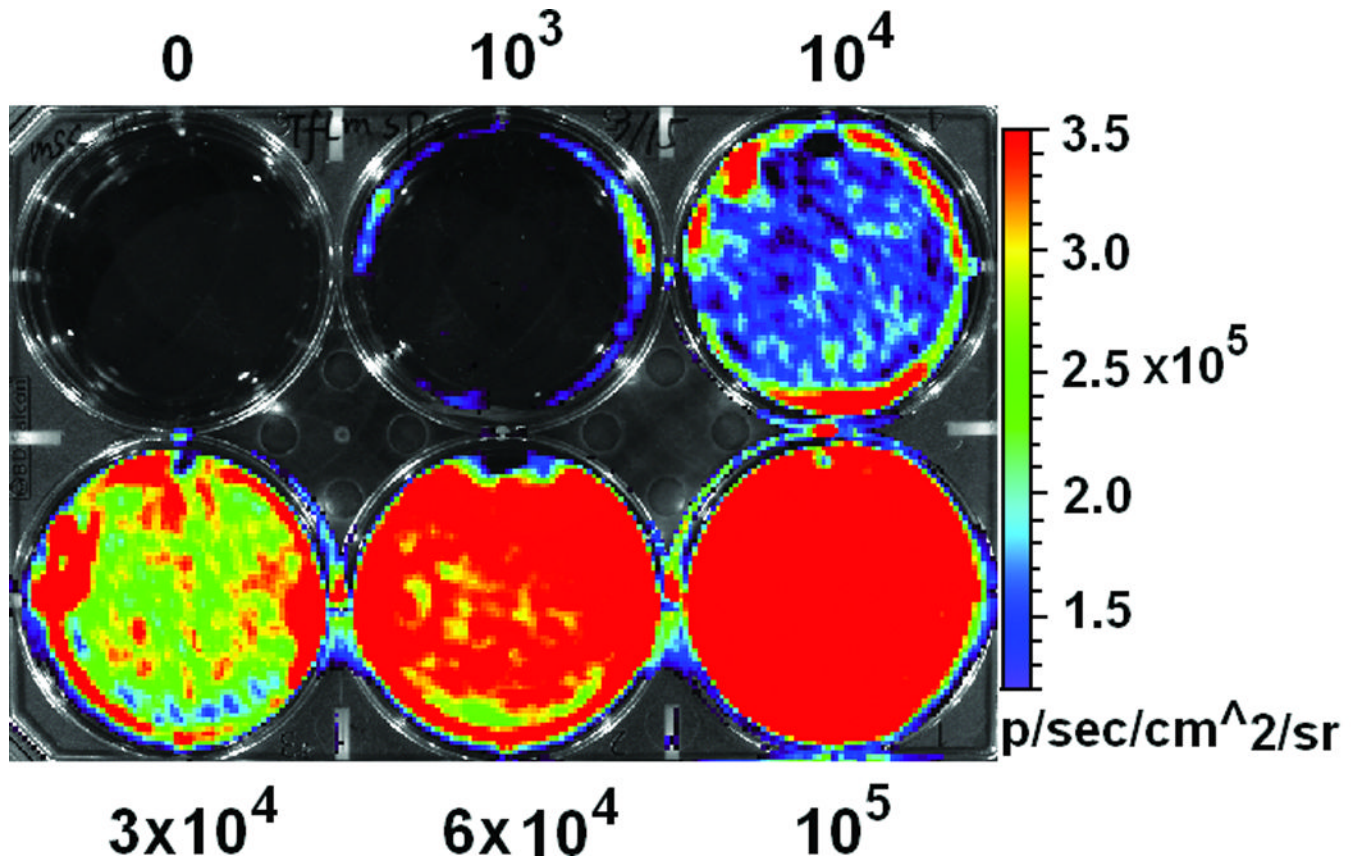








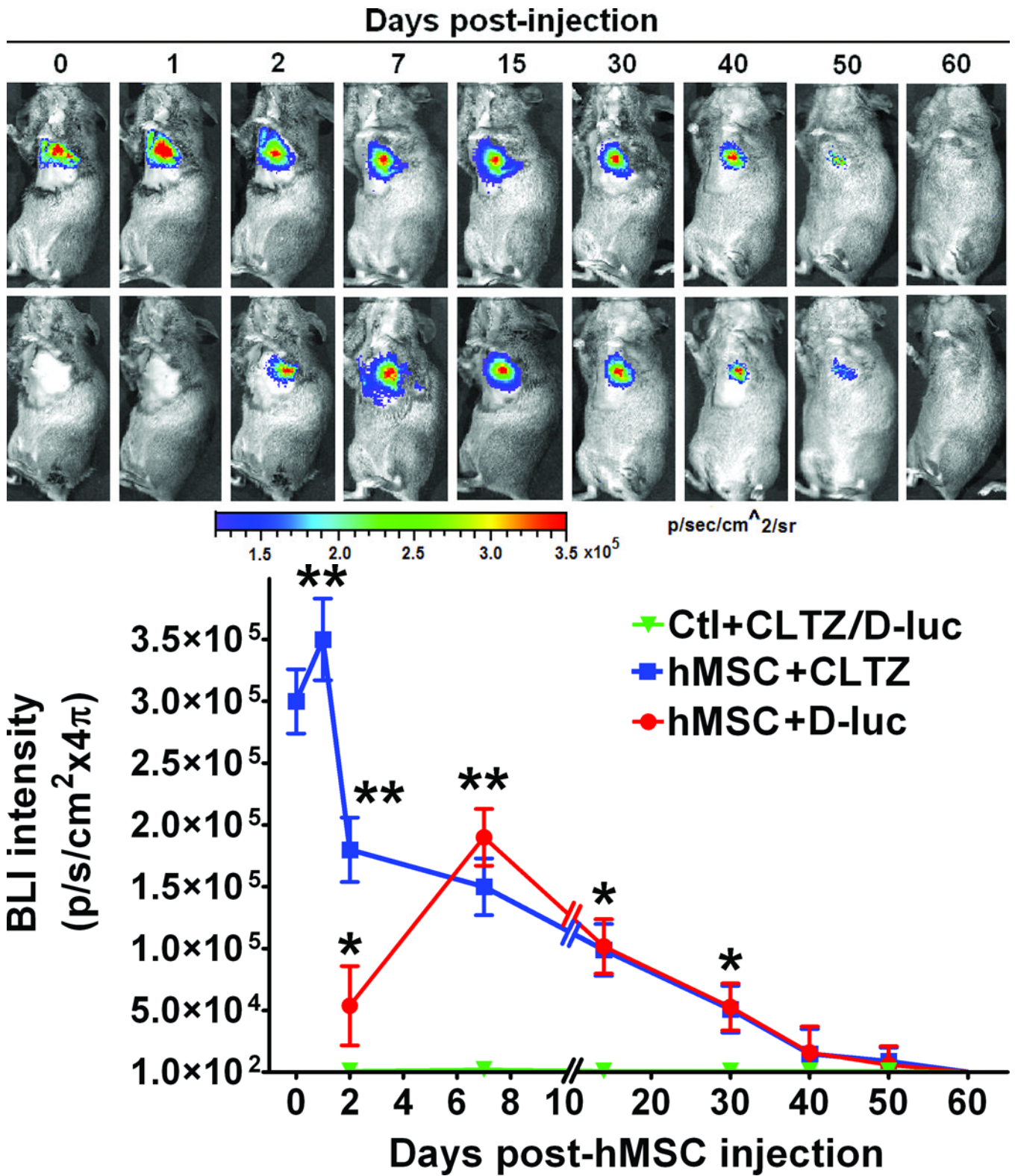




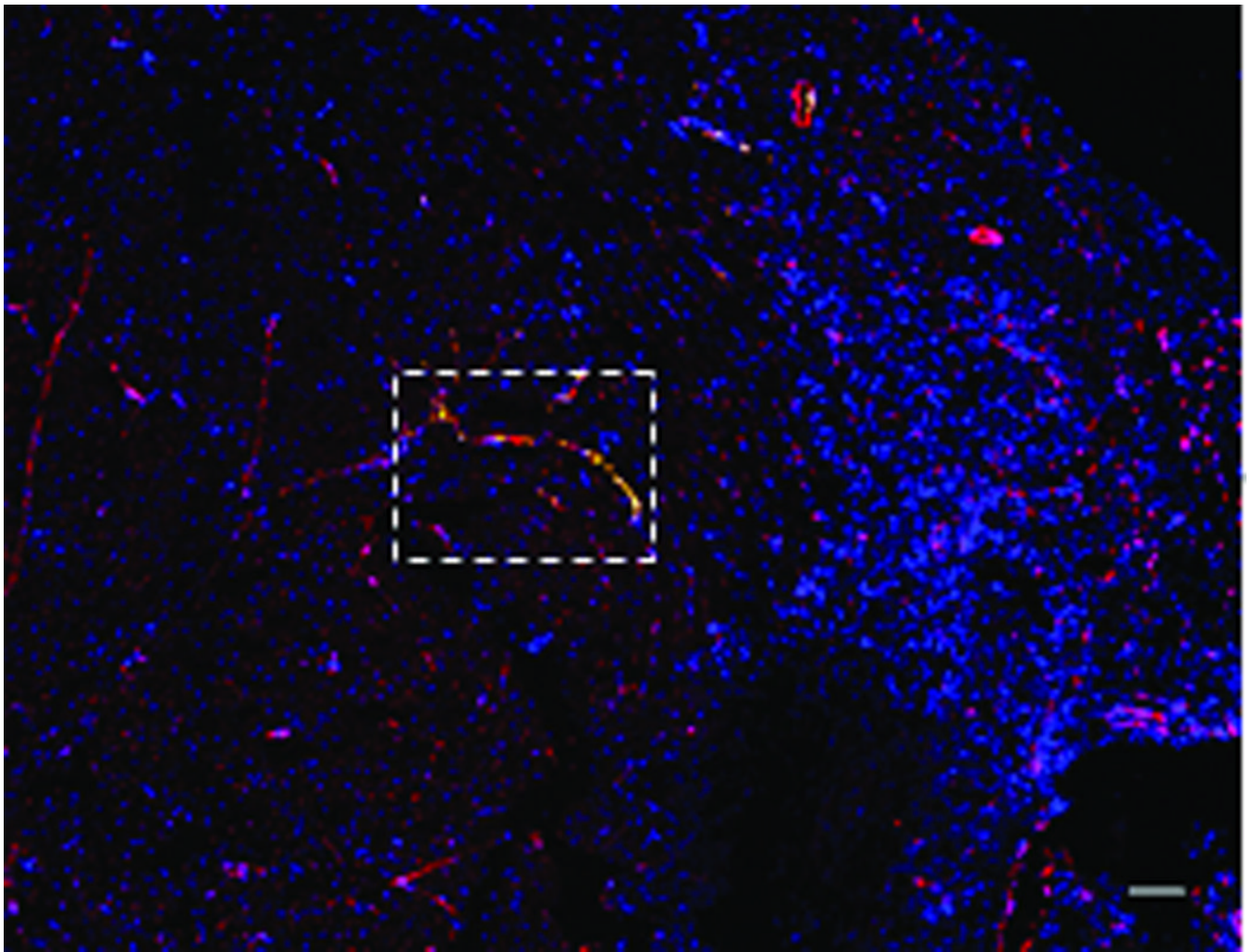
**Figure 1. Validation of endothelial expression of the reporter gene in target cells in vitro**

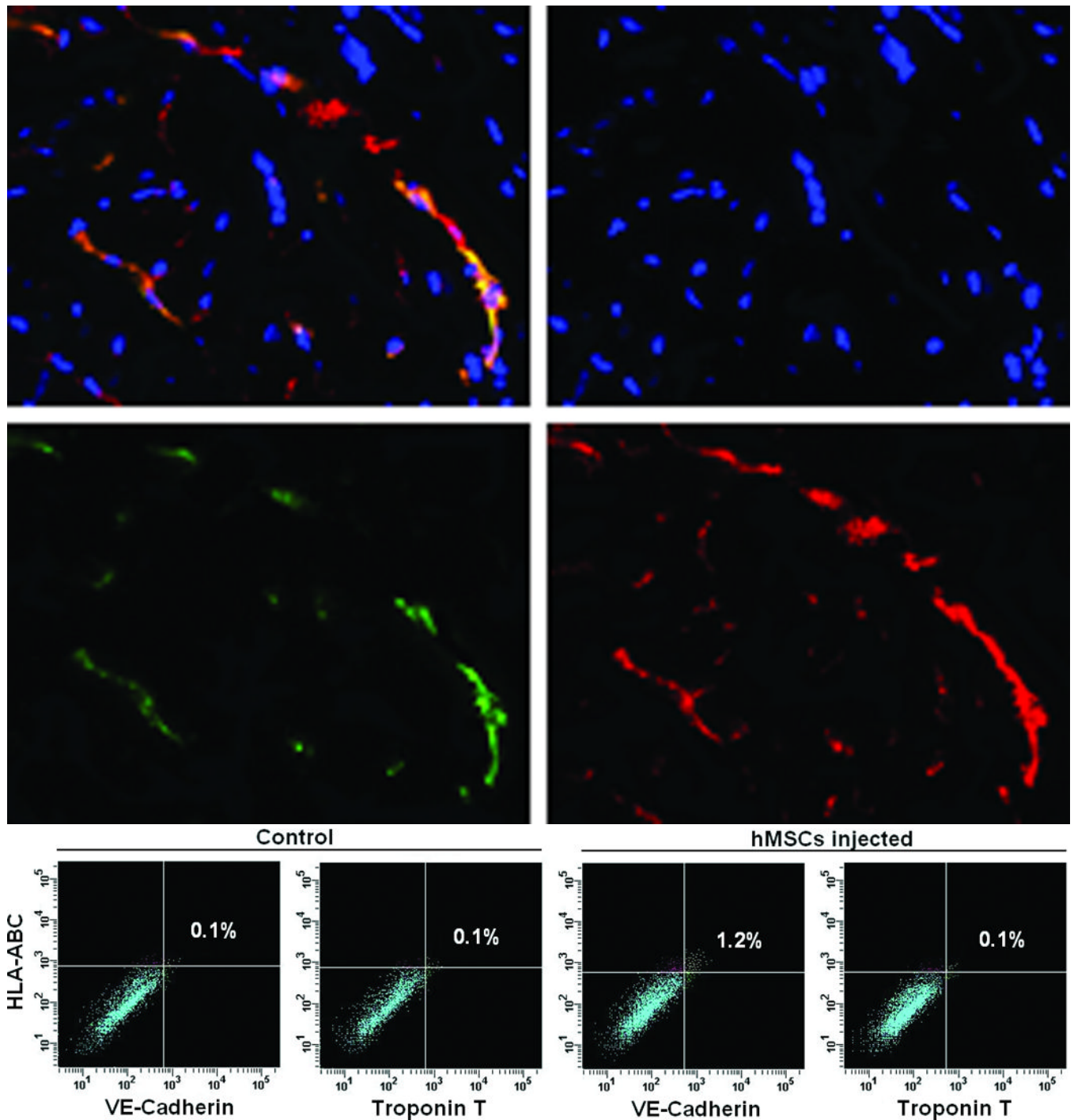
**A.** Schematic representation of lentivector the dual reporter construct. The mCherry-Renilla luciferase (C/r-Luc) fusion reporter gene is driven by the murine stem cell virus (MSCV) constitutive promoter. The eGFP-firefly luciferase (G/f-Luc) fusion reporter gene is driven by the endothelial cell specific promoter, Tie-2. The transcriptional activity of juxtaposed promoters is oppositely directed. **B** and **C.** Representative fluorescent microscopy images illustrate the specific and constitutive expression of reporter genes in mouse endothelial cells (mETCs, positive control) and human mesenchymal stem cells (hMSCs) transduced with lentivirus. Tie-2-driven expression of G/f-Luc in hMSCs was not detected by fluorescence microscopy. Scale bars in B and C, 200  $\mu\text{m}$ . **D** and **E.** Flow cytometry data of transduced mETCs and hMSCs illustrate cell-specific expression of reporter genes. The majority of mETCs express both C/r-Luc and G/f-Luc, whereas most hMSCs express only the MSCV-driven C/r-Luc gene. **F.** In vitro assessment of bioluminescence imaging (BLI) signal in mETCs and hMSCs is shown 72 hours following lentivirus transduction. BLI signal is detected in transduced mETCs with coelenterazine (CLTZ) and D-luciferin (D-Luc) indicating expression of both Tie-2-driven r-Luc and constitutive f-Luc. In contrast, only r-Luc-induced BLI signal is detected in transduced hMSCs. Quantification of the BLI signals (photons/second) is illustrated as a bar graph (bottom). **G.** BLI of graded numbers ( $1 \times 10^3$ – $1 \times 10^5$ ) of hMSCs 48 hours following lentivirus transduction was performed to correlate signal intensity and cell number. Quantification of BLI signal intensity shows a robust correlation between r-Luc activity and the number of transduced hMSCs (bottom). The correlation coefficient,  $r^2$ , is statistically significant ( $p=0.0001$ ).







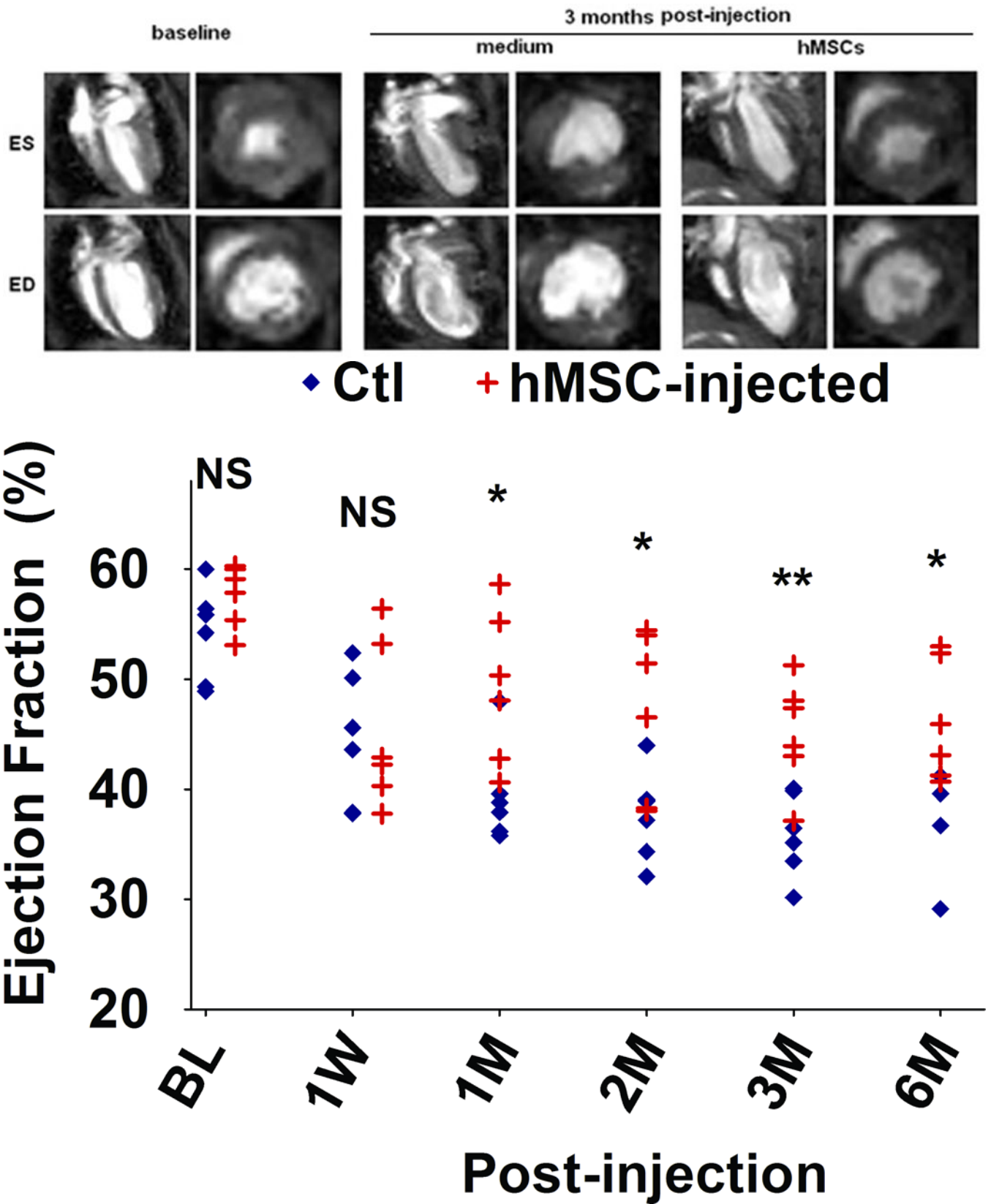




**Figure 2. Persistence and endothelial differentiation of injected hMSCs in vivo**

Acute myocardial infarction (AMI) was induced in a total of 24 SCID mice and mice were subsequently injected (as the time point indicated for respective figure panel) with either transduced hMSCs (hMSC group) or medium (control group, N = 12 per group). In each group, six mice were tracked with BLI to monitor in vivo homing, distribution, and survival duration of injected hMSCs over two months; six mice were sacrificed at two weeks after injection and then hearts were collected. Amongst the latter, three hearts were sectioned for

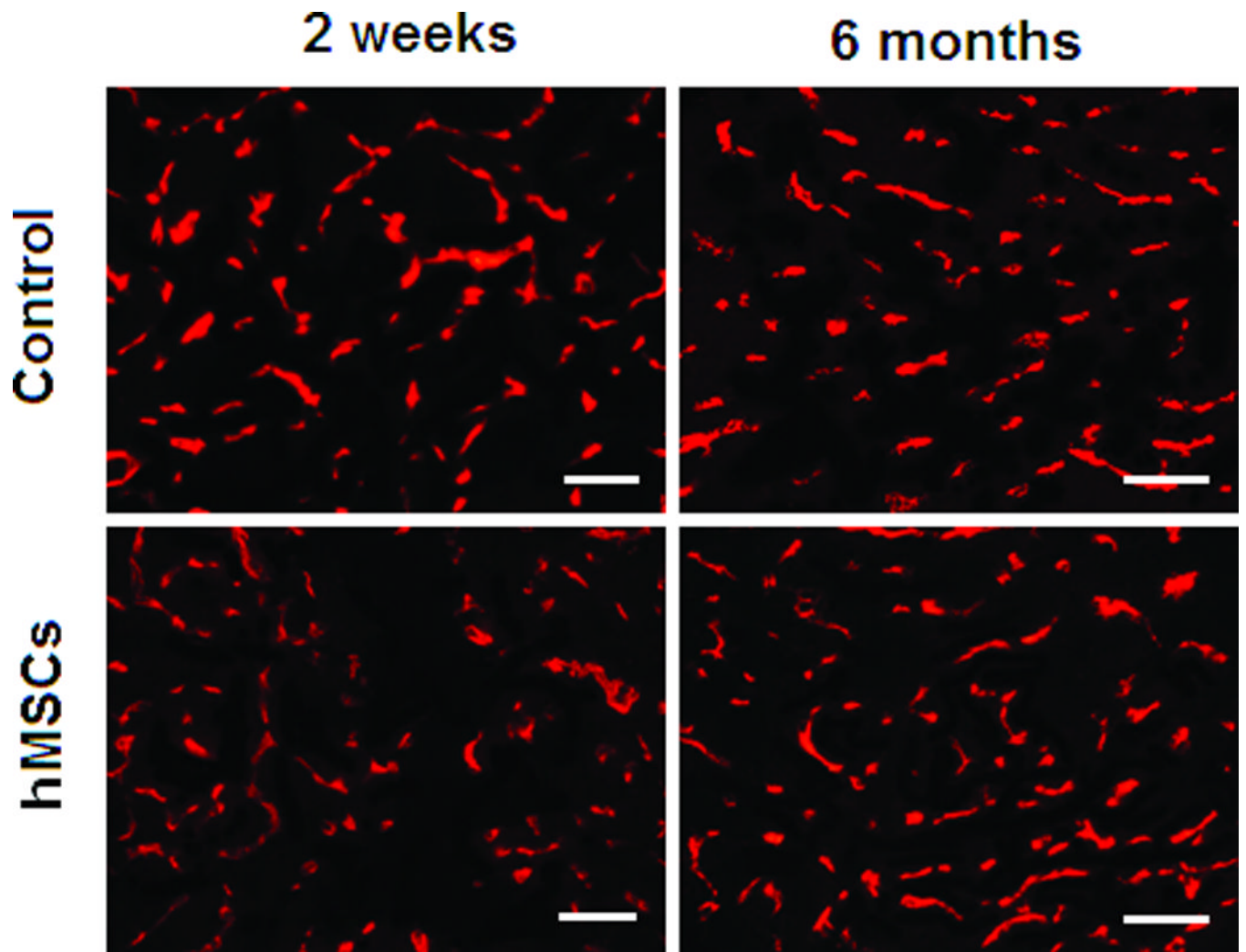
immunohistochemical staining with CD31 and GFP; and the other three hearts were enzymatically digested to get single cell suspension for FACS analysis. **A.** The BLI signals in the heart of a representative mouse were superimposed on photographs of a representative SCID mouse for the indicated time point following injection of hMSCs/medium after AMI. The signals were probed by intraperitoneal injection of CLTZ (upper), or of D-Luc (lower). **B.** Quantitative BLI intensity in SCID mice post-hMSCs/medium injection. BLI intensity was assessed by measuring the photon flux from region of interest (ROI) drawn over the precordium. Repeated-measures ANOVA was used for comparison of hMSCs injection group versus control group at different time points (N = 6 mice per group, \*\* $p < 0.01$  and \* $p < 0.05$ ). **C.** Immunostaining for CD31 and GFP showed the presence of endothelial differentiated hMSCs (GFP<sup>+</sup>) in the vessels of the border zone at 2 weeks following hMSC injection. Scale bar, 200  $\mu\text{m}$ . **D.** Higher magnification of the selection (dotted white square) shown in panel C. Immunostaining of CD31 (red) was performed to detect endothelial cells, and GFP was used to detect the endothelial differentiated hMSCs. Scale bars, 50  $\mu\text{m}$  (N = 3 mice per group). **E.** Representative flow cytometry profile of cells isolated from the heart at 2 weeks post-hMSC injection. The fluorescence intensity of cells stained simultaneously with anti-human HLA-ABC and either anti-cardiac troponin T (to detect cardiomyocytes) or anti-VE-cadherin (to detect endothelial cells) is shown. The percentage of VE-cadherin positive cells was 10-fold higher in hMSC injected mice than that in control mice (N = 3 mice per group).

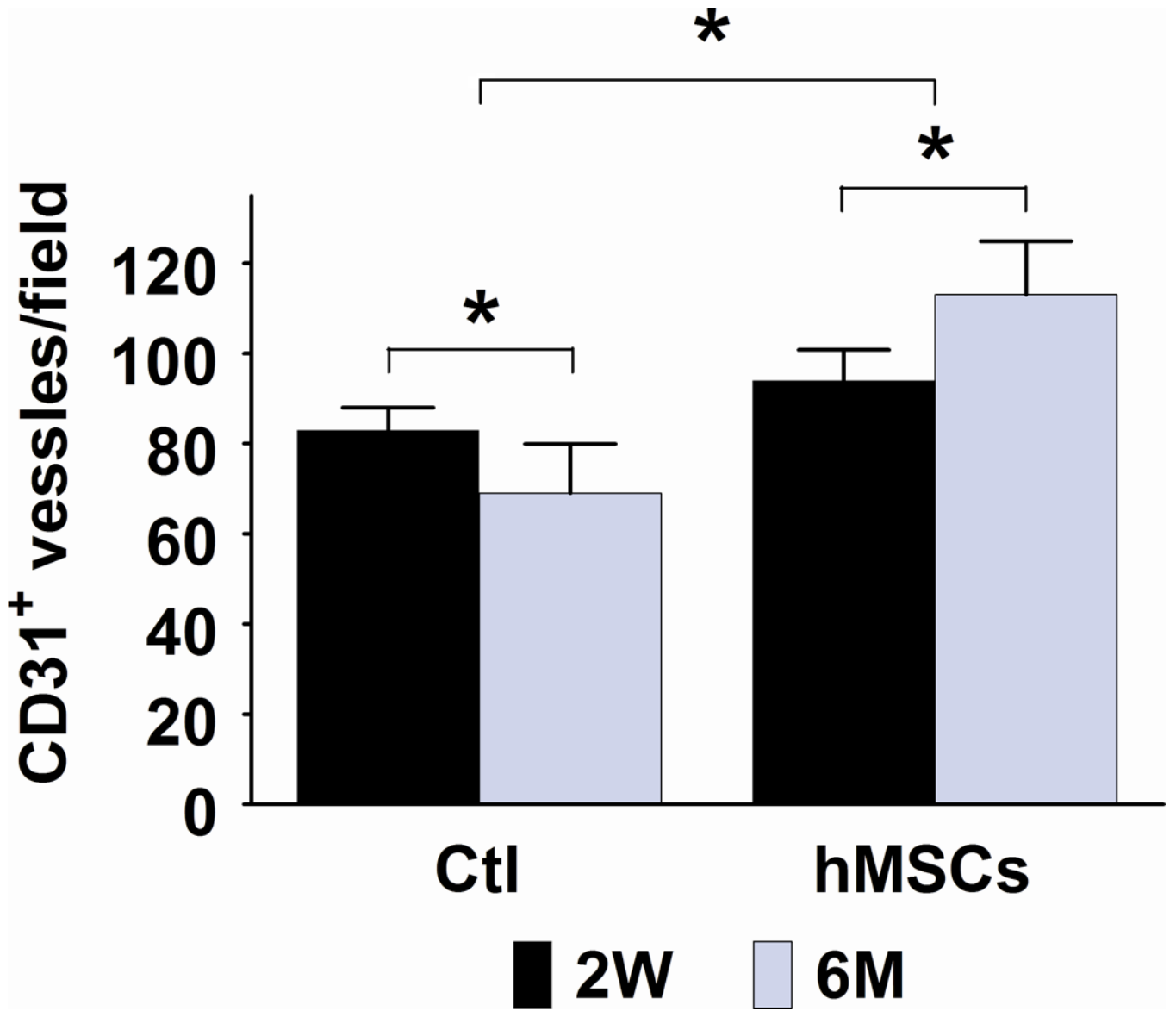


**Figure 3. Injection of hMSCs improves cardiac function, as assessed by cardiac MRI**

**A.** Representative sequential images collected for analysis of the end-systolic (ES) and end-diastolic (ED) volumes from an hMSC-transplanted mouse and a control mouse over a six month period. **B.** Scatter plot showing left ventricular ejection fraction (LVEF) values of individual mice in hMSC-transplanted versus control groups, collected beginning at one day before injection (baseline, BL), one week (W) and continuing over a six month (M) time period after injection. The mean  $\pm$  SE was calculated for each group, and repeated-measures ANOVA was used for comparison of LVEFs between control and hMSCs groups (N = 6 mice per group, NS, not significant; \*\* $p < 0.01$ ; \* $p < 0.05$ ). Beginning at one month after hMSC injection, there was a significant difference in LVEF between groups at each time point.



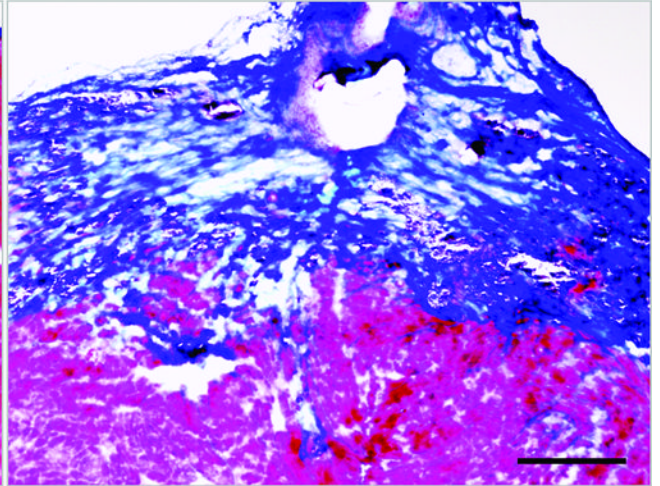
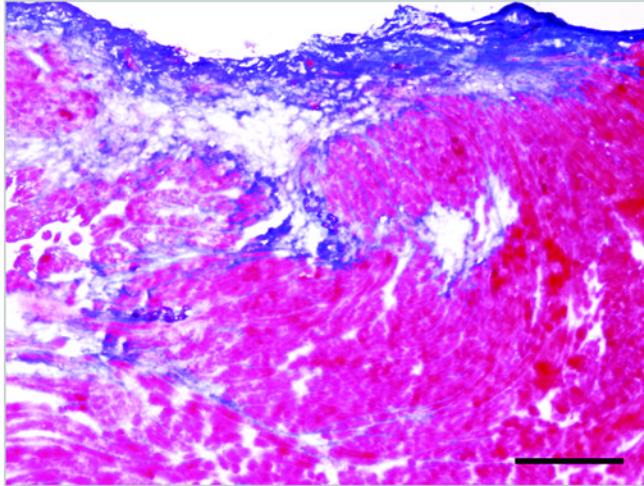




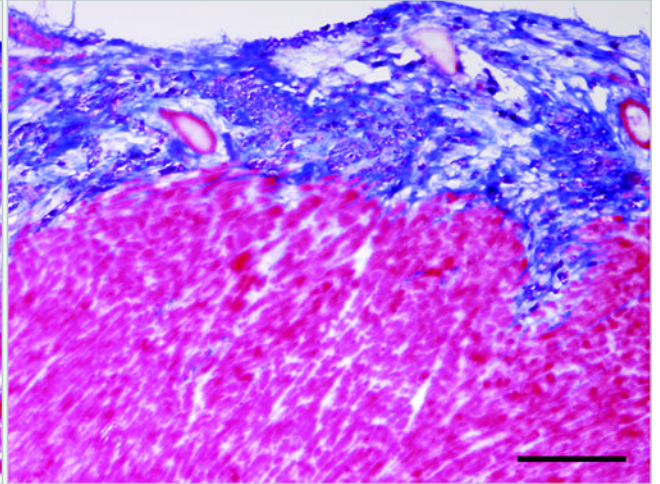
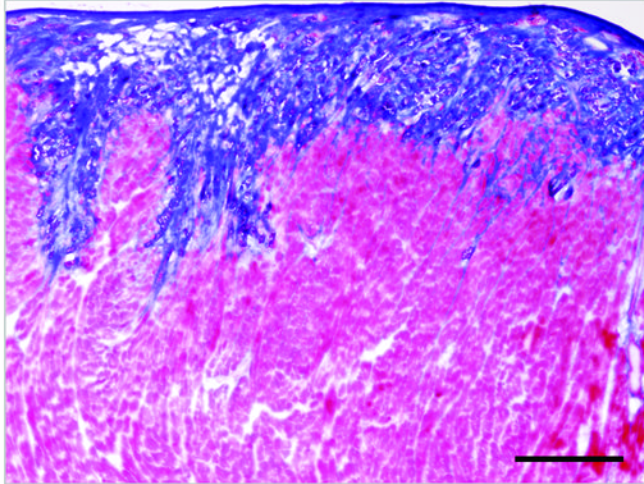
**2 Weeks**

**6 Months**

**Control**



**hMSCs**



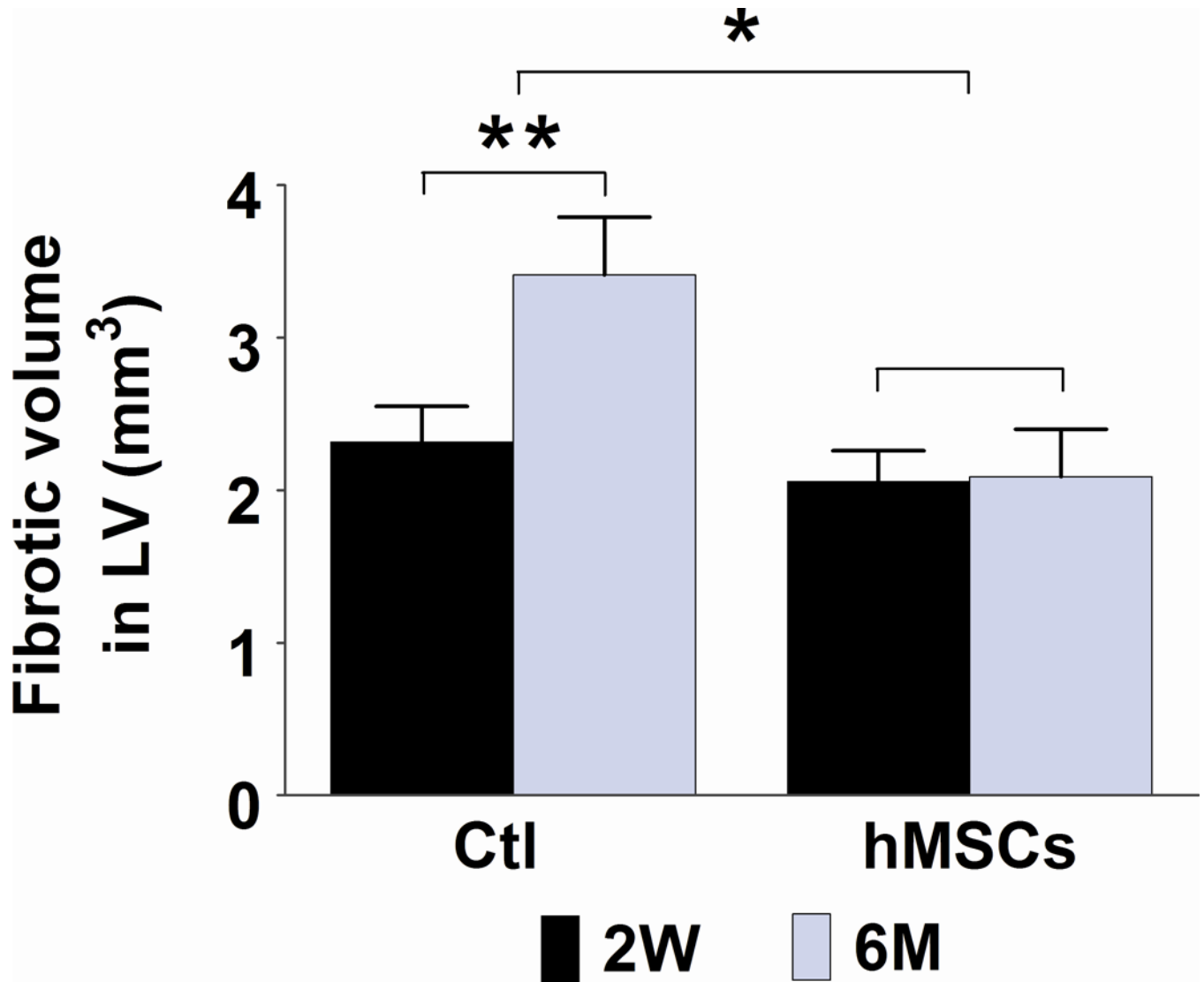


**Figure 4. Injection of hMSCs enhances cardiac angiogenesis and attenuates cardiac fibrosis** **A** and **C**. Representative frozen heart sections from mice two weeks (W) and six months (M) following hMSC or control (medium) injection. Peri-infarct sections were stained with antibody to CD31 to visualize the vessel density (**A**) and stained with Masson trichrome to evaluate fibrosis (**C**). Scale bars, 200  $\mu$ m. **B**. Quantification of CD31<sup>+</sup> cells in peri-infarct sections that are shown in Figure A. The bars represent mean  $\pm$  standard deviation 16 frozen sections per animal. For each section, the number of CD31<sup>+</sup> vessels in 6 fields (400X) was counted and averaged. **D**. Morphometric analysis of cardiac fibrosis was performed as described the methods and elsewhere.<sup>19</sup> The mean  $\pm$  SE was calculated for each group, and the Student's t-test was used for evaluate the differences between the groups (N = 3 mice per group, \*\* $p$ <0.01; \* $p$ <0.05).